

GENERATING QUALITY STRUCTURED CONVEX GRIDS ON IRREGULAR REGIONS*

P. BARRERA-SÁNCHEZ ^{†§}, F. J. DOMÍNGUEZ-MOTA ^{‡¶}
G. GONZÁLEZ-FLORES ^{†§}, AND J. G. TINOCO-RUIZ [‡]

Dedicated to Víctor Pereyra on the occasion of his 70th birthday

Abstract. In this paper, we address the problem of generating good quality grids on very irregular regions, and propose a measure for both the quality of the generated grids and the difficulty of the problem, as well as an efficient algorithm based on the minimization of area functionals to solve it. Using the proposed measure, a preliminary classification of some standard test regions is presented.

Key words. Numerical grid generation, variational grid generation, area functionals, direct optimization method

AMS subject classifications. 65L50, 65M50, 65N50, 78M50, 80M30

1. Introduction. The variational problem of generating structured grids in the plane has been studied in detail in previous papers. There is currently a robust theory regarding area and harmonic functionals, which can be used for the successful gridding of very irregular regions [7, 8, 9, 10]. A deep geometric insight into these functionals is available, as presented in [2] and [1, 3, 5, 6]. Adaptive versions for all these functionals have also been developed [4].

However, a question that arose immediately in these papers is how “good” the generated grids are. To answer it, we must pose a practical definition of quality in the direct optimization method [9, 11]. In the following sections, we provide an intuitive answer motivated mainly by the fact that the areas of the cells in every optimal grid are as close together as possible.

This paper is organized as follows: Sections 1 and 2 discuss the terminology required. Section 3 defines a new scale-independent test for variational grid generation: ϵ -convexity. Section 4 addresses briefly the direct optimization method as proposed by Charakhch’yan and Ivanenko [9]. As an efficient solution to the problem of generating ϵ -convex grids, Sections 5 and 6 introduce the shifted and bilateral functionals $S_{\omega,\epsilon}$ and $B_{\omega,\epsilon}$. Section 7 features the corresponding algorithm. Section 8 addresses the issue of how to measure the quality of grids generated in quite irregular regions. Section 9 presents the numerical tests. Conclusions are presented in Section 10.

2. Discrete structured grid generation problem.

2.1. Continuous grids. The regions on the grid generation problem of interest are simple connected domains Ω in the plane, whose boundaries are closed polygonal positively-oriented Jordan curves. For such regions, the problem can be described as the construction of continuous functions $x(\xi, \eta)$, $y(\xi, \eta)$ to define a one-to-one mapping

$$\mathbf{x} : R \mapsto \Omega \text{ with } \mathbf{x} = (x(\xi, \eta), y(\xi, \eta))$$

from the unit square

$$R = \{(\xi, \eta) | 0 \leq \xi \leq 1, 0 \leq \eta \leq 1\}$$

* Received February 15, 2008. Accepted December 16, 2008. Published online on May 7, 2009. Recommended by José Castillo.

[†]Facultad de Ciencias, U.N.A.M., México (pbs_gfgf@hp.fciencias.unam.mx).

[‡]Facultad de Ciencias Físico Matemáticas, U.M.S.N.H., México (dmota,jtinoco@umich.mx).

[§]Supported by Macroproyecto: Tecnologías para la Universidad de la Información y la Computación.

[¶]Supported by CIC-UMSNH Grant 9.16 and Project CIC/COECyT-Michoacán “Métodos variacionales discretos para la generación numérica de mallas”.

onto the physical region Ω to be gridded in such a way that $\mathbf{x}(\partial\mathbf{R}) = \partial\Omega$.

In practical terms, the discrete structured grid generation problem can be described as the efficient construction of a logically rectangular subdivision of Ω formed by convex quadrilaterals. These subdivisions, as defined in the next section, will be referred to as grids.

It is important to remark that in order to test the robustness of the algorithm presented in Section 7, meshing in this paper is done with a single block.

2.2. Discrete grids. Let us consider a region Ω in the plane, defined by a simple, closed and counterclockwise-oriented polygonal curve γ of vertices $V = \{v_1, v_2, \dots, v_q\}$ (Figure 2.1).

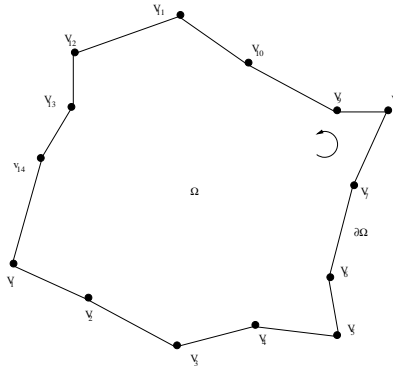


FIGURE 2.1. Example of a region defined by a simple closed polygonal curve.

DEFINITION 2.1. Let m, n be natural numbers with $m, n > 2$. A set of points in the plane

$$G = \{P_{i,j} | 1 \leq i \leq m, 1 \leq j \leq n\}$$

with boundaries

$$L_1(G) = \{P_{i,1} | i = 1, \dots, m\}$$

$$L_2(G) = \{P_{m,j} | j = 1, \dots, n\}$$

$$L_3(G) = \{P_{i,n} | i = 1, \dots, m\}$$

$$L_4(G) = \{P_{1,j} | j = 1, \dots, n\}$$

is called a structured, admissible and discrete grid¹ for Ω , of order $m \times n$, if

$$V \subseteq \bigcup_{i=1}^4 L_i(G).$$

In addition, we will say that G is convex if each one of the $(m-1)(n-1)$ quadrilaterals (or cells) $c_{i,j}$ of vertices $\{P_{i,j}, P_{i+1,j}, P_{i,j+1}, P_{i+1,j+1}\}$, with $1 \leq i < m$ and $1 \leq j < n$, is convex and non-degenerate, except, possibly, in the corner cells.

Hereinafter, $M(G)$ will represent the set of all the admissible grids for Ω according to the previous definition.

The sets $L_1(G)$, $L_2(G)$, $L_3(G)$, and $L_4(G)$ will be referred to as *the sides of the grid boundary* or *the grid sides*, and appear in the definition to emphasize our interest in having

¹With quadrilateral elements.

the same boundary for the region and for the grid. In this sense, from now on, Ω will denote not only the region itself, but also the four sides $L_1(G)$, $L_2(G)$, $L_3(G)$, and $L_4(G)$.

In order to have control over the convexity of the grid cells, it will be of the greatest relevance to consider every grid cell $c_{i,j}$ with vertices $P_{i,j}, P_{i+1,j}, P_{i,j+1}, P_{i+1,j+1}$ as divided into the four oriented triangles $\Delta^{(1)} = \Delta_{i,j}^{(1)}$, $\Delta^{(2)} = \Delta_{i,j}^{(2)}$, $\Delta^{(3)} = \Delta_{i,j}^{(3)}$, and $\Delta^{(4)} = \Delta_{i,j}^{(4)}$ (Figure 2.2).

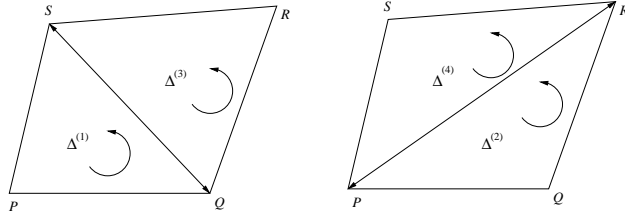


FIGURE 2.2. The four oriented triangles defined by a quadrilateral grid cell.

Let us notice that the orientation of the boundary induces that of the cells and triangles of the cells, inducing a sign on the triangle areas which is the key to finding out whether a grid is convex.

2.3. Important quantities. In order to pose some useful functionals, in this section we introduce two basic triangle-dependent quantities: λ and α . For the oriented triangle with vertices $A, B, C \in \mathbb{R}^2$, these functions are defined as

$$\lambda(\Delta(A, B, C)) = \|A - B\|^2 + \|C - B\|^2, \quad (2.1)$$

where \overline{AB} and \overline{CB} are cell sides and

$$\alpha(\Delta(A, B, C)) = (B - A)^t J_2 (B - C) = 2 \text{ area}(\Delta(Q, P, R)), \quad (2.2)$$

where $\|\cdot\|$ denotes the Euclidean norm and J_2 is the matrix

$$J_2 = \begin{bmatrix} 0 & 1 \\ -1 & 0 \end{bmatrix}.$$

Notice that a grid G is *convex* iff

$$\min\{\alpha(\Delta_q) > 0 | q = 1, \dots, N\},$$

where $N = 4(m - 1)(n - 1)$ is the total number of triangles in G , considering the four triangles in each cell defined by its vertices as mentioned above.

The following three important quantities are related to α :

$$\alpha_-(G) = \min\{\alpha(\Delta_q) | q = 1, \dots, N\}, \quad (2.3)$$

$$\alpha_+(G) = \max\{\alpha(\Delta_q) | q = 1, \dots, N\}, \quad (2.4)$$

$$\overline{\alpha}(\Omega) = \frac{1}{N} \sum_{q=1}^N \alpha(\Delta_q). \quad (2.5)$$

Equation (2.2) yields

$$\sum_{q=1}^N \alpha(\Delta_q) = 4 \text{ Area}(\Omega), \quad (2.6)$$

and thus $\bar{\alpha}$ depends only on Ω and not on a particular G since

$$\bar{\alpha}(\Omega) = \bar{\alpha}(G) = \frac{1}{N} \sum_{q=1}^N \alpha(\Delta_q) = \frac{\text{Area}(\Omega)}{(m-1)(n-1)}. \quad (2.7)$$

For the sake of brevity, α_q and $\alpha(\Delta_q)$ will be used interchangeably in this paper.

3. The ϵ -convexity. As we mentioned before, a grid G is convex iff $\alpha_-(G) > 0$. However, this inequality is neither scale-independent nor a numerically stable test. This is because the problem of generating convex grids in some irregular regions may be ill-posed in the sense that the critical value

$$\epsilon_c(\Omega) = \max \left\{ \frac{\alpha_-(G)}{\bar{\alpha}(\Omega)} \mid G \in M(\Omega) \right\} \quad (3.1)$$

can become be very small.

Nevertheless, this test can be reformulated in a numerically useful way. Since for any convex grid G we have

$$0 < \frac{\alpha_-(G)}{\bar{\alpha}(\Omega)} \leq \epsilon_c,$$

it follows that if we choose $\epsilon > 0$, then any grid G satisfying

$$\epsilon_c \geq \frac{\alpha_-(G)}{\bar{\alpha}(\Omega)} \geq \epsilon$$

is convex. Consequently, the following definition appears in a natural way.

DEFINITION 3.1. *Let ϵ be a positive number. A grid G is ϵ -convex iff*

$$\min\{\alpha(\Delta_q) > \epsilon \cdot \bar{\alpha}(\Omega) \mid q = 1, \dots, N\}. \quad (3.2)$$

This new definition of convexity has proven to be very useful because it is scale-independent, which is a desirable property.

4. Direct optimization method. The basis for the direct optimization method, as developed by Charakhch'yan and Ivanenko [9], is the minimization a suitable function of the form

$$F(G) = \sum_{q=1}^N f(\Delta_q), \quad (4.1)$$

where $f(\Delta_q)$ depends only on the vertices of the triangle Δ_q and N is the total number of triangles of the grid, so that our problem is to find the coordinates of the interior points of the grid G . Thus, a grid G will be represented by a point in n -dimensional space, where the coordinates are the x and y coordinates of the interior points of the grid.

In this context, the discrete variational grid generation problem can be posed as a large-scale optimization problem in the following way:

PROBLEM 4.1. *Solve*

$$G^* = \arg \min_{G \in M(\Omega)} \sum_{q=1}^N f(\Delta_q)$$

over the set of admissible grids $M(\Omega)$ for a region Ω and a given ϵ , in such a way that G^* is ϵ -convex.

We must emphasize that the adequate selection of f is the key to generating an ϵ -convex grid in an efficient way, as will be shown in the following sections.

Using equation (3.2), the following can be shown:

- If $\epsilon > \epsilon_c$, Problem 4.1 has no solutions.
- In contrast, if $\epsilon \leq \epsilon_c$, Problem 4.1 has solutions.
- If $\epsilon \approx \epsilon_c$, the problem might be very difficult for the numerical optimization.

5. Convex area functionals with barriers. In this section, we address the issue of designing efficient functionals to solve Problem 4.1. First, though, we review some important functionals.

5.1. Ivanenko's harmonic functional. The first effective functionals for the generation of convex harmonic grids on quite irregular regions were developed by A. A. Charakhch'yan and S. A. Ivanenko [8, 9]. A beautiful insight into these functionals can be found in [10].

These authors rewrote the harmonic functional proposed by Winslow [16] in a variational setting [9], and discretized it to obtain a function of the inner grid points similar to the expression (4.1) presented in the preceding section, with f given as

$$f(\Delta_q) = \frac{\lambda(\Delta_q)}{\alpha(\Delta_q)}. \quad (5.1)$$

They then minimized the corresponding functional by means of a Newton iteration.

It is easy to prove that Ivanenko's functional attains its minimum in the set of convex grids for a region due to the pole in f and the relations between α and λ [8]. However, for fixed boundary points the minimization process required a rather complicated formula to get an initial convex grid [9].

5.2. Tinoco's quasi-harmonic functional. Later, Tinoco [6] developed a new quasi-harmonic functional with an easier initialization by choosing f as

$$f_\omega(\Delta_q) = \frac{\lambda(\Delta_q) - 2\alpha(\Delta_q)}{\omega + \alpha(\Delta_q)}, \quad (5.2)$$

where ω is a parameter that allows the use of non-convex initial grids by setting

$$\omega > -\alpha(\Delta_q), \quad q = 1, \dots, N.$$

For both Ivanenko's and Tinoco's functionals, the optimal grids generated were only required to satisfy the scale-dependent convexity test. This caused numerical instability in some irregular regions.

5.3. The functional S_ω . Ivanenko's and Tinoco's functionals feature poles as barriers, a fact that can be disadvantageous and cause instability if small values of α are produced on some irregular regions. In order to avoid the use of poles as barriers, Barrera and Domínguez-Mota comprehensively analyzed the properties of a family of continuous discrete area functionals (i.e., with no explicit dependence on λ) with *soft* barriers [2], and proved the following theorem:

THEOREM 5.1. *Let $f : \mathbb{R} \rightarrow \mathbb{R}$ be a C^2 convex, strictly decreasing and nonnegative function, and define $F : \mathbb{R}^N \rightarrow \mathbb{R}$ by*

$$F(G) = \sum_{q=1}^N f(\alpha_q).$$

Let Ω be a polygonal regions for which there exists a convex grid G_0 . Then it is possible to find a real number t for the scaled region $t\Omega$ such that the optimization problem

$$\min\{F(G)|G \in M(t\Omega)\},$$

where $M(t\Omega)$ is the set of admissible grids for $t\Omega$, has a solution \hat{G} that satisfies $\alpha_-(\hat{G}) > 0$.

Despite the simplicity of these results, $F(G)$ still lacks the scale-independent property required to work robustly on very irregular non-convex regions. Even though the shift required in Theorem 5.1 in order to generate ϵ -convex grids is almost automatic, it is also important enough to deserve a new subsection.

5.4. The shifted functional $S_{\omega,\epsilon}$. An efficient solution to Problem 4.1 was proposed by Barrera and Domínguez-Mota [3], who realized that one of the main conclusions of Theorem 5.1, the positivity of the least value of α of the optimal grid, could be restated in terms of a shifted inequality. Indeed, the theorem itself can be easily restated to generate ϵ -convex grids in the following way:

THEOREM 5.2. *If f is a C^2 strictly decreasing convex and bounded below function such that $f(\alpha) \rightarrow 0$ as $\alpha \rightarrow \infty$, then*

$$S_{\omega,\epsilon}(G) = \sum_{q=1}^N f(\omega\alpha(\Delta_q) - \epsilon\bar{\alpha}(G)) \quad (5.3)$$

considered as the objective function in the optimization Problem 4.1, is minimized by ϵ -convex grids for $\omega > 0$ large enough.

One must notice that, as a straightforward consequence of this theorem, for numerical purposes very economical choices for f , such as

$$\psi(\alpha) = \begin{cases} 1/\alpha, & \alpha \geq 1 \\ (\alpha - 1)(\alpha - 2) + 1, & \alpha < 1, \end{cases}$$

can be used.

The ϵ -convex grids generated by minimizing $S_{\omega,\epsilon}$ with (5.4) have been reported by the authors in previous papers, for instance [2]. In many irregular regions, the presence of cells with relatively large values of $\alpha_+(G)$ has been observed. This often slows down the optimization process when generating ϵ -convex grids with good area control.

6. The bilateral functional $B_{\omega,\epsilon}$. It is straightforward to address the requirement of decreasing $\alpha_+(G)$ and propose another functional to solve Problem 4.1. In [5], Tinoco proposed a way to apply his adaptive area functional “twice” in order to control large and small values of α simultaneously by using

$$f_{\omega_1,\omega_2}(\Delta_q) = \frac{1}{\omega_1 + \alpha(\Delta_q)} + \frac{1}{\omega_2 - \alpha(\Delta_q)}, \quad (6.1)$$

where ω_1 and ω_2 are parameters introduced to increase the lower values of α and decrease the larger values of α , respectively.

It is easy to conclude that the same strategy proposed in [2] can be applied twice in the same fashion. The functional S_{ω} was designed to increase the lower α values in a grid by means of the parameter ω . Now, to avoid very large cell areas, it is convenient to consider a “reflection” of S_{ω} in order to create a second control barrier. Consequently, it is possible to define a new functional with two barriers, the bilateral B_{ω} , as

$$B_{\omega,\epsilon}(G) = \sum_{q=1}^N \left(\psi(\omega(\alpha_q - \epsilon\bar{\alpha}(G))) + \psi\left(\frac{\omega}{c}(\alpha_0 - \alpha_q)\right) \right), \quad (6.2)$$

where $\omega > 0$, $c > 0$ is a fixed parameter to control the relative rigidity between the two barriers in (6.2), and $\alpha_0 > \bar{\alpha}(G)$ is another fixed parameter to control large cell areas.

If α_0 is adequately selected, then every minimizer of $B_{\omega,\epsilon}$ is attained deep within the first orthant, i.e., for numerically positive values of α . Thus, the left barrier in $B_{\omega,\epsilon}$ takes care of convexity, and the right one improves grid quality.

Some interesting grids generated for several regions will be shown in the following sections. The first step to accomplish this task is to briefly describe a useful algorithm related to the direct optimization method.

7. Generation algorithm. In the present section, we show a practical way to use the results that have been discussed so far. It is important to consider the following facts:

- The numerical optimization process produces an ϵ -convex grid close to an actual optimal grid.
- Numerical optimization requires convergence criteria. Such decisions are made by considering the gradient norm and the relative functional change in the algorithm.
- In practice, it is convenient to scale Ω to satisfy the condition,

$$\bar{\alpha}(\Omega) = 1,$$

which immediately implies

$$\alpha_-(G) \leq 1 \leq \alpha_+(G).$$

In this way, the following algorithm can be used to generate convex grids:

ALGORITHM 7.1. *Convex grid generation with $B_{\omega,\epsilon}$*

1. Choose initial values for $tolf$, $tolg$, ω , $\tau > 1$, $ITERMAX$ and $\epsilon > 0$.
2. Generate an initial grid G_0 and scale it to satisfy $\bar{\alpha} = 1$.
3. Choose $\alpha_0 > 1$ and $c > 0$.
4. Solve the optimization problem

$$\hat{G} = \arg \min_{G \in M(\Omega)} \{B_{\omega,\epsilon}(G)\} \quad (7.1)$$

until

$$\|\nabla B_{\omega,\epsilon}(\hat{G})\| < tolg,$$

or

$$\|B_{\omega,\epsilon}(\hat{G}) - B_{\omega,\epsilon}(G_0)\| < tolf \cdot \|B_{\omega,\epsilon}(G_0)\|,$$

or $ITERMAX$ has been reached.

5. If $\alpha_-(\hat{G}) > \epsilon$, an ϵ -convex grid has been generated and we are done; elseif $ITERMAX$ was reached, no convex grid has been found and we are done; else we set $\omega \leftarrow \tau\omega$, $G_0 \leftarrow \hat{G}$, and go back to step 3.

It is important to observe that the factor τ and the initial value for t in the algorithm are quite arbitrary, although it is clear that different choices mean different numbers of iterations in the optimization process.

TABLE 9.1
Parameters for the optimization.

Parameter	Value
tol_f	10^{-7}
tol_g	10^{-5}
ω	10.0
τ	2.000
$ITERMAX$	1000
$\min \varepsilon$	10^{-4}
c	0.5
α_0	$\max(0.9 \cdot \alpha_+(G), 1.0)$

8. Quality grid measurement in terms of area. It is very important to observe that the reciprocal of ϵ_c , which we will denote by

$$\kappa = \frac{1}{\epsilon_c} = \frac{\bar{\alpha}(G)}{\max\{\alpha_-(G) | G \in M(\Omega)\}}, \quad (8.1)$$

can be understood as a condition number for Ω .

Indeed:

- κ is a function only of m , n , and the geometries of V and Ω .
- κ is scale-independent.
- $\kappa \geq 1$.
- If all the values of α in a grid G are equal, then $\kappa = 1$.

These reasons make κ a good parameter for measuring grid quality in terms of area. However, it must be estimated, since ϵ_c is unknown a priori.

A fast estimate of κ can be obtained by defining the quality ratio q for a convex grid G :

$$q(G) = \frac{\alpha_-(G)}{\bar{\alpha}(G)}. \quad (8.2)$$

As before, q is scale-independent, and for rectangular grids, $q = 1$. As $\alpha_-(G) \rightarrow 0$, $q \rightarrow 0$.

Since

$$q \leq \epsilon_c = 1/\kappa,$$

one can see that a large “condition number” for a region corresponds to a low quality of the grids generated for it.

9. Numerical experiments. In order to calculate q and obtain a practical approximation to κ , it is practical to use the α values for the optimal grids of $B_{\omega, \varepsilon}$, since this functional was precisely designed to reduce the interval $[\alpha_-(G), \alpha_+(G)]$ as much as possible [3].

In the numerical tests presented below, the test regions were scaled to satisfy $\bar{\alpha}(G) = 1$, which led to $\varepsilon \in [0, 1]$ for the generation algorithm of Section 7. The optimization step was carried out with Newton-like methods for large-scale problems [13, 17]. The parameters used for the algorithm and the optimization process are summarized in Table 9.1. Since the value ϵ_c is unknown a priori, an initial value of $\varepsilon = 0.1$ was used, and once an ε -convex grid was generated, we set $\varepsilon \leftarrow \varepsilon + 0.1$ until no ε -convex grid was generated.

We applied Algorithm 7.1 to twelve test regions that have been frequently used in the literature related to grid generation, grouped in two sets:

- I. Airfoil, Annulus, Chevron, Dome, Plow, and Swan (Figure 9.1).

II. Cat, Great Britain, Havana, Mexico, Sigma, and Ucha (Figure 9.2).

The first group has appeared in tests for many different methods. These regions have been gridded with algebraic, differential, and other methods [12]. The second group includes very irregular regions, for which most of the algebraic and differential methods fail, but that can be gridded successfully with the direct optimization method [2].

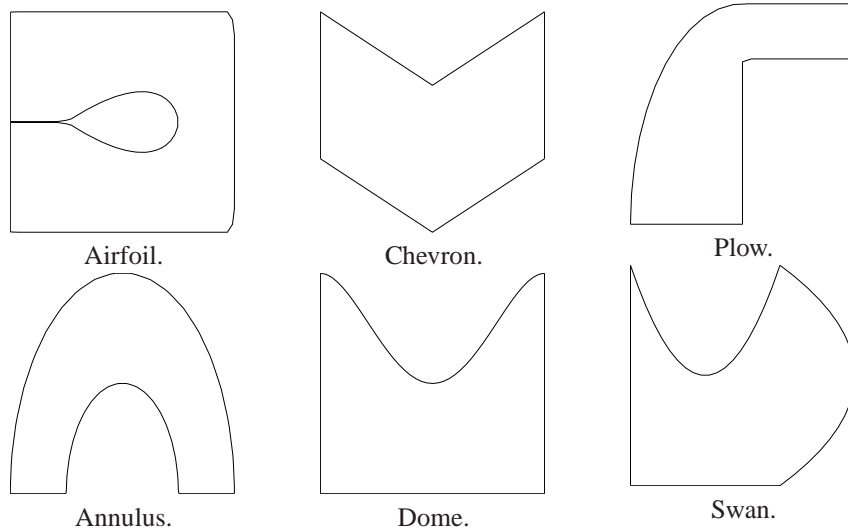


FIGURE 9.1. Test regions. Set I.

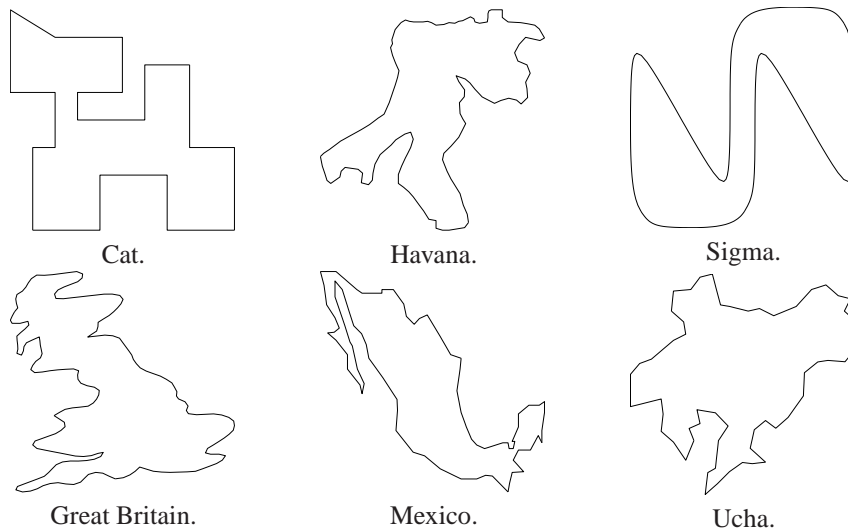


FIGURE 9.2. Test regions. Set II.

The initial grids for both groups, generated with Algorithm 7.1 using $\varepsilon = 0.01$, were convex. Three different grid sizes were considered: 31, 51, and 71 points per side. In Tables 9.2, 9.3, and 9.4, there is a summary of α_- , α_+ , and q^{-1} , sorted as a function of the latter. Note that, due to normalization, $q = \alpha_-$. These tables also include the standard deviation

TABLE 9.2
Results for the test regions (31 points per side).

Region	n	α_-	α_+	q^{-1}	STD
Chevron	31	0.99680	1.00320	1.00321	0.00146
Dome	31	0.95149	3.88970	1.05098	0.12797
Airfoil	31	0.83361	1.34550	1.19960	0.08345
Ucha	31	0.75006	5.87921	1.33323	0.52299
Havana	31	0.73399	4.44630	1.36242	0.53137
Swan	31	0.70219	2.04255	1.42412	0.13046
Plow	31	0.67201	2.38785	1.48807	0.37279
Cat	31	0.65603	3.94373	1.52432	0.49377
Great Britain	31	0.40264	3.75619	2.48361	0.57017
Annulus	31	0.32333	1.28390	3.09282	0.03798
Sigma	31	0.25462	1.80445	3.92742	0.45769
Mexico	31	0.22156	7.98021	4.51345	0.76749

TABLE 9.3
Results for the test regions (51 points per side).

Region	n	α_-	α_+	q^{-1}	STD
Chevron	51	0.99759	1.00240	1.00242	0.00022
Dome	51	0.94695	2.61970	1.05602	0.09769
Ucha	51	0.87677	3.64730	1.14055	0.31298
Airfoil	51	0.86640	2.41650	1.15420	0.00179
Havana	51	0.83030	4.81440	1.20438	0.39002
Cat	51	0.82346	4.01970	1.21439	0.41991
Plow	51	0.73384	2.84615	1.36269	0.25332
Swan	51	0.68971	2.32260	1.44988	0.09442
Annulus	51	0.66670	1.97820	1.49993	0.03798
Great Britain	51	0.50205	3.74210	1.99183	0.42759
Sigma	51	0.23926	2.69440	4.17955	0.47527
Mexico	51	0.09105	7.38490	10.98298	0.52611

(STD) for the values of α for each one of the final grids generated, and just like in the first test, the values for the four fixed corners are excluded.

Let us notice that, in general, if a region is irregular or strongly nonconvex, its values of α are more spread and grids of lower quality are obtained. But though some quality is lost in the values of the standard deviation of α indicate that even for most of the irregular regions, large deviations occur only locally.

In terms of the values of q one can conclude that, as expected, regions in set I are generally simpler for the grid generation problem than those in set II. It is important to mention that q^{-1} is, by definition, an upper bound of the condition number κ proposed in Section 8. Recalling that κ is always greater than one, the reciprocal of the quality ratio provide us with useful information about the geometrical difficulty of a region in the context of the grid generation problem of our interest.

9.1. Smoothness control. It is important to emphasize that the main problem of this paper was to pose a measure of the quality of a grid in terms of its values of α . This is quite natural in the context of the theory of the convex area functionals [2]. However, one must acknowledge that there are some other useful considerations in judging the quality of

TABLE 9.4
Results for the test regions (71 points per side).

Region	n	α_-	α_+	q^{-1}	STD
Chevron	71	0.99360	1.00641	1.00644	0.00207
Ucha	71	0.90307	2.38464	1.10733	0.18025
Airfoil	71	0.86282	2.23778	1.15899	0.03909
Havana	71	0.85723	4.90527	1.16655	0.31738
Cat	71	0.85212	3.94372	1.17354	0.34611
Plow	71	0.81788	1.99423	1.22267	0.09273
Swan	71	0.70301	1.97769	1.42245	0.06934
Annulus	71	0.68653	1.05089	1.45660	0.01914
Dome	71	0.66388	2.64157	1.50630	0.04420
Great Britain	71	0.51647	4.04164	1.93622	0.36091
Mexico	71	0.11298	6.80687	8.85112	0.40978
Sigma	71	0.09018	1.50805	11.08893	0.30015

TABLE 9.5
Results for the grids with smoothness control, $n = 50$.

Region	n	α_-	α_+	q_2^{-1}
Havana	0.50	0.79931	4.33295	1.25108
Great Britain	0.75	0.25245	5.08705	3.96120
Sigma	0.75	0.20150	1.83115	4.96268
Mexico	0.90	0.10140	7.38493	9.86217

a grid. One of the most important is smoothness, which can be achieved with Winslow’s functional [4, 8].

In this sense, some of the area grids presented in the previous section might be considered coarse. However, coarseness is not a major problem using the direct optimization method. It is possible to use the length functional given by

$$L(G) = \sum_{q=1}^N \lambda(\Delta_q)$$

as a smoother. Thus, with a linear convex combination between $B_{\omega,\epsilon}(G)$ and $L(G)$, one can generate both convex *and* smooth grids [14]. Just as an example, let us consider the last four grids with 71 points per side, modified by minimizing

$$\sigma \cdot B_{\omega,\epsilon}(G) + (1 - \sigma) \cdot L(G).$$

The figures for this grid are shown in Table 9.5. The corresponding grids are included in Figures 9.3, 9.4, and 9.5. These grids speak by themselves: some quality in terms of area has been lost, but the gain in smoothness is quite evident.

10. Conclusions and future work. We have introduced a measure of the quality of a structured grid in terms of area, as well as a new bilateral area functional to generate quality convex grids. According to the results obtained, it is possible to conclude that the direct optimization method is very well suited to solve this problem on very irregular regions.

In a future paper, other quality measures based on some other geometrical properties as smoothness and orthogonality will be reported, as well as some results for the analogous 3D

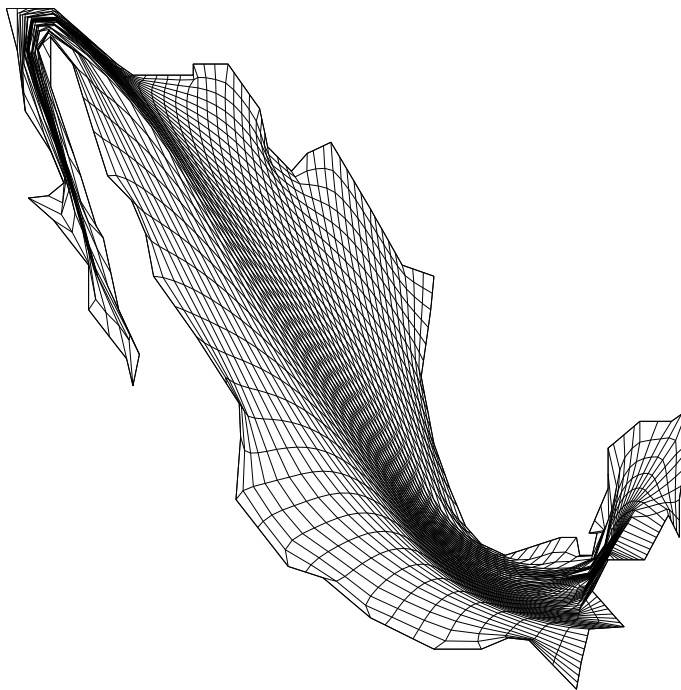


FIGURE 9.3. A grid for Mexico with smoothness control.

problem for which, up to our knowledge, a practical computational test for convexity of cells in structured grids might not be as intuitive and simple as the one given by equation (3.2).

The functional addressed in this paper, as well as some other useful area and smoothness functionals, are currently included in the software UNAMALLA [15].

Acknowledgements. We want to thank Intercambio Académico of UNAM and the “Macroproyecto: Tecnologías para la Universidad de la Información y la Computación”, CIC-UMSNH Grant 9.16, and Project CIC/COECyT-Michoacán “Métodos variacionales discretos para la generación numérica de mallas” for the financial support for this work.

Many thanks due to the reviewers of this paper for their always valuable suggestions and comments.

REFERENCES

- [1] P. BARRERA-SÁNCHEZ, L. CASTELLANOS, AND A. PÉREZ-DOMÍNGUEZ, *Métodos variacionales discretos para la generación de mallas*, DGAPA-UNAM México, 1994.
- [2] P. BARRERA-SÁNCHEZ, F. J. DOMÍNGUEZ-MOTA, AND G. F. GONZÁLEZ-FLORES, *Robust discrete grid generation on plane irregular regions*, *Comput. Math. Math. Phys.*, 43 (2003), pp. 845–854.
- [3] ———, *Area functionals for high quality grid generation*, in Proceedings of the 4th. International Congress on Numerical Methods in Engineering and Applied Sciences, M. C. Suárez, S. Gallegos, S. Botello, M. Moreles, J. J. Pérez Gavilán, F. Zárate, F. Domínguez, and M. X. Rodríguez, eds., Sociedad Mexicana de Métodos Numéricos en Ingeniería y Ciencias Aplicadas, Morelia, Mexico, 2007.
- [4] ———, *Adaptive discrete harmonic grid generation*, *Math. Comput. Simulation*, 79 (2009), pp. 1792–1809.
- [5] P. BARRERA-SÁNCHEZ AND J. G. TINOCO-RUIZ, *Area functionals in plane grid generation*, in Proceedings of the 6th. International Conference on Numerical Grid Generation in Computational Field Simulation, M. Cross, B. K. Soni, J. F. Thompson, J. Hauser, and P. R. Eiseman, eds., International Society of Grid Generation, London, 1998, pp. 293–302.

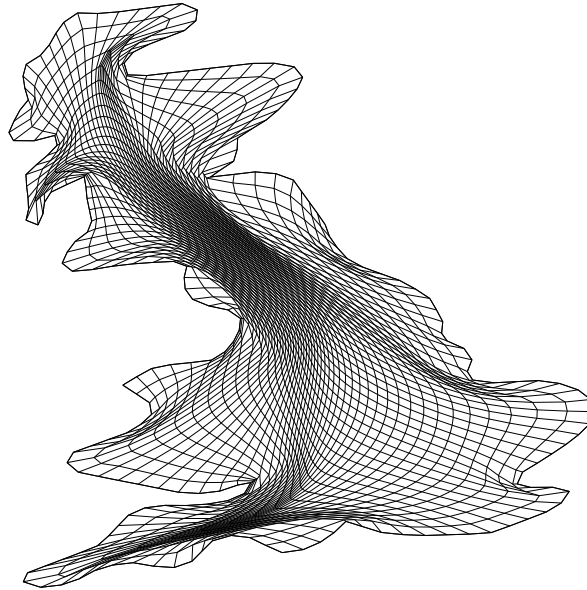


FIGURE 9.4. A grid for Great Britain with smoothness control.

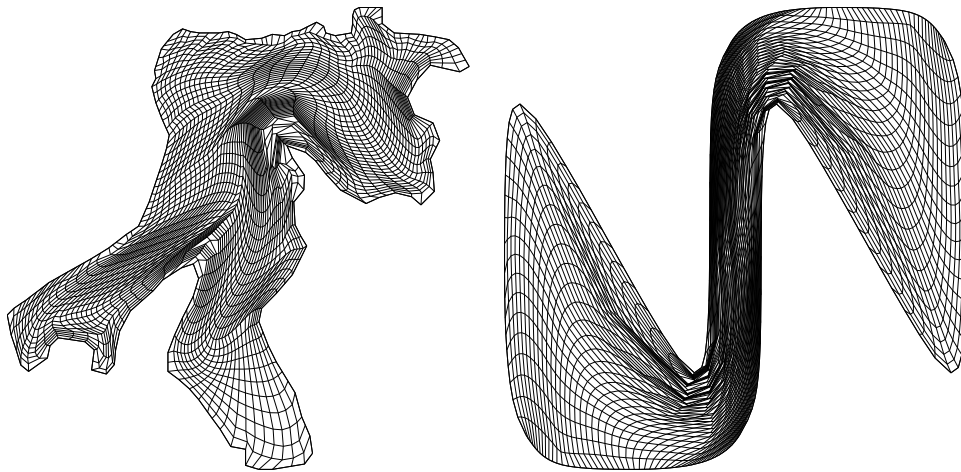


FIGURE 9.5. Grids for Havana and sigma with smoothness control.

- [6] ———, *Smooth and convex grid generation over general plane regions*, Math. Comput. Simulation, 46 (1998), pp. 87–102.
- [7] J. E. CASTILLO, ed., *Mathematical Aspects of Numerical Grid Generation*, Frontiers in Applied Mathematics, SIAM, Philadelphia, 1991.
- [8] A. A. CHARAKHCH'YAN AND S. A. IVANENKO, *A variational form of the Winslow grid generator*, J. Comput. Phys., 135 (1997), pp. 385–398.
- [9] ———, *Curvilinear grids of convex quadrilaterals*, Comput. Math. Math. Phys., 28 (1998), pp. 126–133.
- [10] S. A. IVANENKO, *Harmonic Mappings*, CRC Press, Boca Ratón, Florida, 1999, ch. 8, pp. 8.1–8.41.
- [11] P. KNUPP AND N. ROVIDEAUX, *A framework for variational grid generation: Conditioning the Jacobian matrix with matrix norms*, SIAM J. Sci. Comput., 21 (1999), pp. 2029–2047.
- [12] P. KNUPP AND S. STEINBERG, *Fundamentals of grid generation*, CRC Press, Boca Ratón, Florida, 1992.
- [13] C. . LIN AND J. J. MORÉ, *Newton's method for large-scale bound constrained optimization problems*, SIAM

- J. Optim., 9 (1999), pp. 1100–1127.
- [14] S. STEINBERG AND P. J. ROACHE, *Variational grid generation*, Numerical Methods for Partial Differential Equations, 2 (1986), pp. 71–96.
- [15] *UNAMALLA: An automatic package for numerical grid generation*.
Available at <http://www.matematicas.unam.mx/unamalla>.
- [16] A. M. WINSLOW, *Numerical solution of the quasilinear poisson equations in a nonuniform triangle mesh*, J. Comput. Phys., 2 (1966-67), pp. 149–172.
- [17] C. ZHU, R. H. BYRD, AND J. NOCEDAL, *Algorithm 778: L-BFGS-B: FORTRAN routines for large-scale bound-constrained optimization*, ACM Trans. Math. Software, 23 (1997), pp. 550–560.